

Nanoscale

Accepted Manuscript



This is an *Accepted Manuscript*, which has been through the Royal Society of Chemistry peer review process and has been accepted for publication.

Accepted Manuscripts are published online shortly after acceptance, before technical editing, formatting and proof reading. Using this free service, authors can make their results available to the community, in citable form, before we publish the edited article. We will replace this *Accepted Manuscript* with the edited and formatted *Advance Article* as soon as it is available.

You can find more information about *Accepted Manuscripts* in the [Information for Authors](#).

Please note that technical editing may introduce minor changes to the text and/or graphics, which may alter content. The journal's standard [Terms & Conditions](#) and the [Ethical guidelines](#) still apply. In no event shall the Royal Society of Chemistry be held responsible for any errors or omissions in this *Accepted Manuscript* or any consequences arising from the use of any information it contains.

Sandwich type Plasmonic Platform for MEF using Silver Fractals

Sangram. L. Raut^{a*}, Ryan Rich^b, Tanya Shtoyko^c, Ilkay Bora^d, Bo W. Laursen^d, Thomas Just Sørensen^d, Julian Borejdo^b, Zygmunt Gryczynski^{a,b}, Ignacy Gryczynski^{b*}

In this report, we describe a plasmonic platform with silver fractals for metal enhanced fluorescence (MEF) measurements. When a dye containing surface was brought into contact with silver fractals, a significantly enhanced fluorescence signal from the dye was observed. Fluorescence enhancement was studied with the *N*-methyl-azadioxatriangulenium chloride salt (Me-ADOTA.Cl) in PVA films made from 0.2 % PVA (w/v) solution spin-coated on a clean glass coverslip. The Plasmonic Platforms (PP) was assembled by pressing together silver fractals on one glass slide and a separate glass coverslip spin-coated with a uniform Me-ADOTA.Cl in PVA film. In addition, we also tested the ADOTA labeled human serum albumin (HSA) deposited on a glass slide for potential PP bioassay applications. Using the new PP, we could achieve more than 20-fold fluorescence enhancement (bright spots) accompanied by decrease in fluorescence lifetime. The experimental results were used to calculate the extinction (excitation) enhancement factor (G_A) and fluorescence radiative rate enhancements factor (G_r). No change in emission spectrum was observed for a dye with and without contact with fractals. Our studies indicate that this type of PP can be a convenient approach for constructing assays utilizing metal enhanced fluorescence (MEF) without the need for depositing the material directly on metal structures platforms.

Introduction

Noble metals like silver and gold has found numerous applications in fluorescence field. Starting from very small sub-nanometer scale silver/gold nanoclusters[1, 2, 3] to micron size deposited metallic nanostructures[4, 5] has been topics of continued research efforts in biochemical and material sciences. Metal enhanced fluorescence (MEF) is one such area where deposited metal surfaces are being put to use for enhancing fluorescence signals and developing sensitive assays. Colloidal nanoparticles, nanoprisms, nanocubes, octahedron, nanorods, island films, wires, and fractals are few nanostructures used for such MEF studies[6, 7, 8][7]. Localized surface plasmon resonance (SPR) property of noble metal nanoparticles and nanostructures have been studied extensively and provide attractive approaches to drastically improve fluorescence based detection.

Electrochemically deposited silver fractals are attractive and are being used for MEF applications. Such fractals are known to give about 100 fold fluorescence enhancements [9, 10, 11]. Fluorescence enhancements on the silver fractals is primarily an effect of two processes; (1) enhancement of local electromagnetic field from the excitation light that provides a higher excitation rate for chromophores localized in the enhancement region and, (2) the interaction of excited fluorophores with localized surface plasmons in nearby metallic nanostructures that enhance radiative rate and results in rapid radiation of the excitation energy into free space.

Extensive efforts have been directed towards synthesizing different morphological patterns of metal structures due to their different effect on fluorescence enhancement yields[12, 13, 14]. However, limited efforts have been put into experimenting with plasmonic platform assemblies where metallic structures and investigated materials are independently deposited on separate surface. Here we show PP based on silver fractals that gives comparable fluorescence enhancements to the conventional layout with materials-on-metal-structures PP assembly, when the metallic structure is pressed onto the top surface of the deposited material. Observation of fluorescence enhancements on metallic structures is an obvious phenomenon to fluorescence community, however the approach that we used in this manuscript of making a sandwich of the dye surface and PP is

new and less explored area and can be utilized to increase the dynamic range of existing intensity based assays. This particular methodology can be easily adapted to the existing coverglass slide based assays and sensitivity of commercially available such assay platforms can be increased

Material and Methods

Chemicals

All chemicals and materials were used as received. The water used for all solutions and washings was Millipore grade with > 18.2 M Ω resistivity. Me-ADOTA.Cl was prepared as previously described [15] while ADOTA-NHS (butyric acid derivative) was synthesised accordingly to established procedures[16].

Synthesis of Silver Fractals

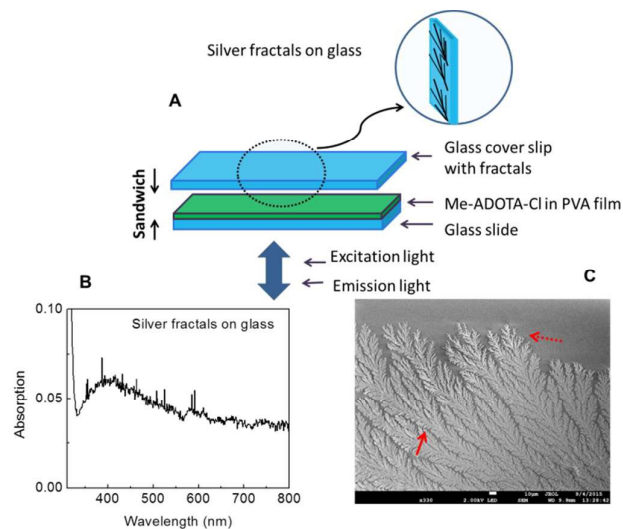


Figure 1: A) Schematic of plasmonic platform B) Absorption of silver fractals on glass C) SEM image of silver fractals on glass. Small white scale bar is 10 μ M.

Silver fractals were prepared on glass cover slips in a similar manner as above. Briefly, two microscope slides (30 mm X 25

mm) were thoroughly washed with Alconox soap, wiped with isopropanol, and rinsed with distilled water. A glass cover slip (20 mm X 20 mm) was soaked in concentrated sulfuric acid for at least 30 min and rinsed with deionized water. The glass cover slip was inserted between the two microscope slides. Two pieces of silver foil (10 mm X 20 mm X 1 mm each) were inserted between the glass cover slip and the top microscope slide and held about 15 mm apart. The sandwich structure was held together with electrical tape. The gap between the glass cover slip and the microscope slide was filled with deionized water. A dc potential of 10 Volt was applied between the two silver foil electrodes. The silver fractal-like structures growth was carried out until the silver fractals were easily seen by the naked eye. Then the fractals in the sandwiched structure were left to dry overnight. The sandwiched structure was disassembled, and the cover slip with fractals was stored to

The sample was prepared by spin coating an aqueous solution of the dye Me-ADOTA.Cl (1 μ M) in 0.2% PVA in DI water (w/v) onto a clean glass coverslip which gives about 30nm high film [17]. The PP was assembled as shown in Figure 1, by putting in contact two parts: sandwiching a Me-ADOTA-Cl covered glass coverslip and a glass slide having silver fractals. Glass cover-slip was brought in contact with silver fractal platform by adding a drop of mineral oil/glycerol on it which ensured they remain together for duration of the measurement. The fluorescence enhancement factor is distance dependent; however, in this report the distance between the dye and silver fractals was not controlled.

Microscopy Measurements

A confocal MicroTime 200 (Picoquant GmbH, Germany) system coupled with an Olympus IX71 microscope was used to obtain time resolved images. Fluorescence photons were gathered from different places of on the sample using 60x water immersed objective (N.A 1.2, Olympus). A 500-nm long-pass filter with additional two 488 R long-pass filters (Shemrock) were applied to remove scattered light. A pulsed laser (470nm-LDH-P-C470B) with repetition rate 20MHz was used as a light source. Fluorescence photons were collected with using a photon counting module (SPCM=AQR-14, Perkin Elmer) with processing accomplished by the PicoHarp300 time correlated single photon counting (TCSPC) module. Data analysis was performed using a SymPhoTime (5.2.4) software package.

Results and Discussion

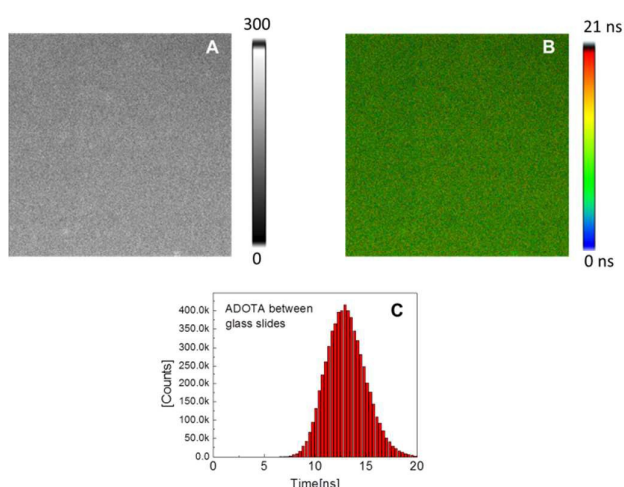


Figure 2: A) 20 X 20 μ m Intensity image of ADOTA between glass coverslips B) 20 X 20 μ m FLIM image of ADOTA between glass coverslips C) Lifetime histogram of ADOTA.

dry in a Petri dish.

Spectra Measurements

Absorption spectra were measured on Cary 50 spectrometer (Varian Inc.). Steady state emission measurements were done using modular Ocean Optics USB spectrometer.

Protein Labelling

Small volume of ADOTA-NHS ester in DMF (less than 5% by volume) was added to a HSA solution in 100mM bicarbonate buffer. The molar ratio of protein to dye was adjusted to 1:5. After 4 hrs of gentle mixing/shaking of the sample, it was passed through the Sephadex-G25 5 mL column to separate the unreacted probe and labelled HSA protein. Labelled protein was used in preparing drop coated plasmonic platform assembly as below.

Film Preparation and Plasmonic Platform (PP) Assembly

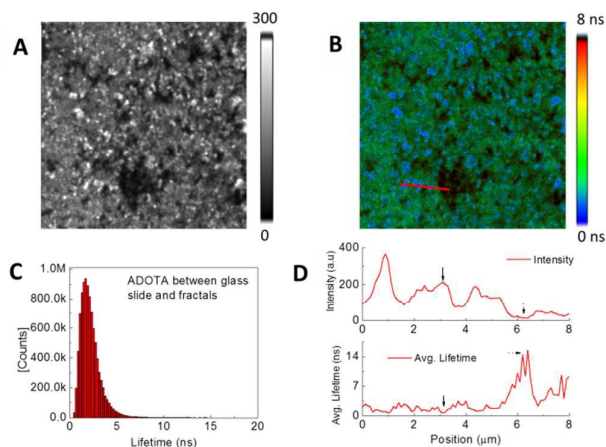


Figure 3: A) 30 X 30 μ m Intensity image of ADOTA between glass coverslip and silver fractals B) 30 X 30 μ m FLIM image of ADOTA between glass coverslip and silver fractals C) Lifetime histogram of ADOTA between glass coverslip and silver fractals D) Intensity and lifetime profile of a red line from FLIM image.

The majority of the metal enhanced fluorescence studies in the literature are done by coating a homogenous layer of

fluorophore solutions directly on to metallic/plasmonic surfaces [11, 18, 19, 20, 21, 22, 23, 24]. Previously, we have used silver fractals to show enhancements where the ADOTA dye was directly deposited on to metallic surface [25]. In this study, for fluorescence enhancement measurements, the samples were prepared in a different configuration, as shown in Figure 1. Figure 1 shows the schematic of the PP assembly. Dye solution (in 0.2% PVA) was spin coated on a glass coverslip so as to get the thin film with uniform dye distribution. This coverslip was brought in contact with fractals containing glass coverslip using drop of glycerol/mineral oil which ensured close contact between two surfaces. Absorption/extinction spectrum of fractals in Figure 1B shows peak around 400 nm suggesting Surface Plasmon Resonance. This spectrum indicates asymmetric shape of deposited silver since the absorption maxima for small particles is expected to be around 380 nm. Figure 1C shows the SEM image of the silver fractals on glass. Areas of thin and thick deposition of silver are clearly visible in the image.

Figure 2 A shows the 20 X 20 μm confocal intensity image of ADOTA between two glass coverslips. The dye is distributed uniformly on the glass surface. The average fluorescence lifetime (Figure 2 B) of the ADOTA here was 12.8 ns (multi-exponential). Figure 2 C shows the lifetime histogram of ADOTA sample on glass with lifetime from about 8 ns to 20 ns having relatively broad distribution. The reduced lifetime on glass (12.8 ns) compared to bulk solution (~ 20 ns) is expected due to quenching by oxygen, freely diffusing into the thin film, and possible aggregation in the concentrated sample in small area [26,27] Moreover, when ADOTA sample was placed in contact with fractals non-uniform fluorescence intensity enhancement was observed as shown in Figure 3 A. Two populations of enhanced fluorescence are clearly visible namely bright white spots and relatively uniform grey areas. These two population are represented by two different lifetimes in the FLIM image (Figure 3B) shown by green and blue color. The signal from black areas (void of fractals) was

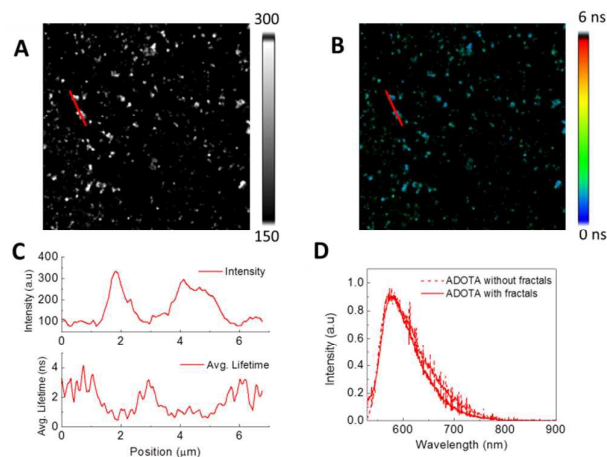


Figure 4: A) 30 X 30 μm Intensity image of ADOTA between glass coverslip and silver fractals B) 30 X 30 μm FLIM image of ADOTA between glass coverslip and silver fractals C) Intensity and lifetime profile of a red line from FLIM image D) Emission spectra of ADOTA with and without fractals.

about 15 counts and used to calculate the average enhancement in different areas. The average enhancement in green color (FLIM image) or grey area (intensity image) was ~ 6 times while the enhancement in blue color (FLIM image) or white spots (intensity image) was ~ 24 times. The fluorescence lifetime distribution from the FLIM image is shown in the Figure 3C with narrow distribution. Most of the dye population has lifetime shorter than 5 ns suggesting strong Radiative Decay Engineering (RDE) effect. The effect of fractals on increased fluorescence intensity and decreased lifetime is shown by intensity and lifetime profile of a red line drawn in FLIM image (Figure 3D). The enhanced intensity can be seen from 0 to 5.5 μm while the lifetime is less than 3 ns in that range. On the other hand, lifetime is about ~ 14 ns where there are no fractals as shown by the dashed arrows. This lifetime number is well compared to lifetime we recovered for ADOTA between two glass slides (Figure 2).

To gain further understanding on enhancement in this case, we re-scaled the image in figure 3A from 150 to 300 counts. This image is shown in Figure 4A with corresponding lifetime image in Figure 4B. Figure 4C shows the intensity and lifetime profile of the red line. The enhancement factor on bright spots is ~ 24 times and the lifetime in those areas is around 0.7 ns, while the enhancement factor around bright spots is ~ 6 times where lifetime is about 3.5 ns. Higher enhancement appears to be from the thick deposition of silver while lower one corresponds to thin metallic surfaces. Such thin (red dotted arrow) and thick (red solid arrow) metal areas are visible in figure 1C. Such enhancement is dependent on amount of silver deposited on glass has been observed previously as well [10]. Figure 4 D shows the normalized emission spectrum of ADOTA on glass with and without contact with fractals. We did not see any change in the peak emission of ADOTA in those spectra.

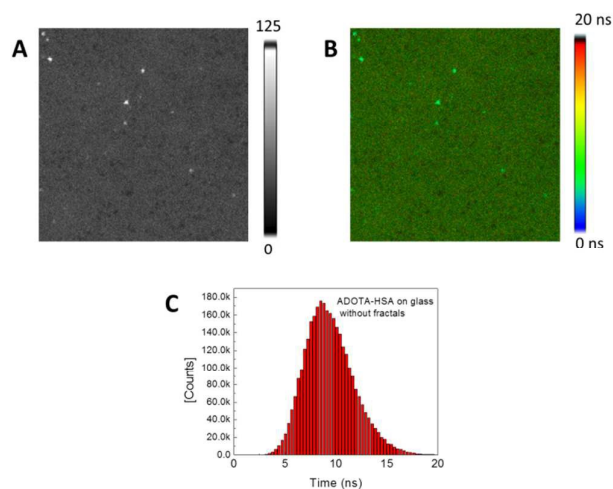


Figure 5: A) 30 X 30 μm Intensity image of ADOTA labeled HSA. B) 30 X 30 μm FLIM image of ADOTA labeled HSA Lifetime distribution in image A. C) Lifetime distribution histogram of ADOTA-HSA on glass.

Due to the direct application of MEF studies to antigen-antibody immunoassays, we tested the applicability of this new PP using ADOTA labeled HSA (ADOTA-HSA). Figure 5 A and B shows the intensity and FLIM image of a monolayer of ADOTA-HSA on plain glass along with lifetime histogram in Figure 5 C. Average fluorescence lifetime was found to be 8.6 ns (heterogeneous multi-exponential decay) on the plain glass where ADOTA appears to be quenched on protein surface. ADOTA is known to get quenched on protein surfaces from previous studies [16] mainly due to the electron transfer from amino acids such as tryptophan, tyrosine, histidine and methionine. Moreover, when this plain glass slide with ADOTA was brought in contact with the fractals, clear fluorescence enhancements were seen in the areas of silver fractals. Figure 6 A and B shows the intensity and FLIM image of ADOTA-HSA in contact with fractals. Figure 6 D shows the lifetime and intensity profile along the red line drawn in 6B. It is visible that the lifetime of ADOTA is shorter where there is enhanced emission intensity and longer at the places void of silver fractals. The average signal from the areas void of fractals was ~ 10 counts and was used to calculate the enhancement

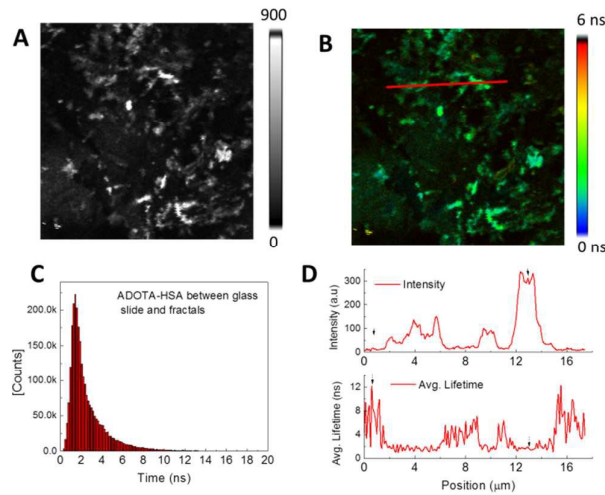


Figure 6: A) 30 X 30 um intensity image of ADOTA labeled HSA put together with fractals. B) 30 X 30 um FLIM image of ADOTA labeled HSA put together with fractals. C) Lifetime distribution

factor. Enhancement is over 20 times in bright spots and the lifetime is shortened by about 5.7 times. Figure 6 C shows the lifetime histogram from image 6A where average lifetime appears to be ~ 1.5 ns.

Theoretical Model. Change in fluorescence intensity could be due to increased excitation efficiency (we called enhanced excitation or enhanced absorption cross section[29, 30] or modification in radiative rate, k_F or/and nonradiative rate, k_{nr} . In typical fluorescence experiments that do not involve plasmonic effects observed change in fluorescence intensity is due to the nonradiative rate modification[31]. However in the presence of metallic nanostructure all rates including enhanced excitation can be altered. In the previous work we have studied all these effects in more details[32, 33]. It was evident that excitation enhancement and radiative rate enhancement are working on much longer distances that

nonradiative rate enhancement[34, 35, 36]. Typically range of quenching by metallic nanostructure is limited to couple of nanometers while enhancement rates may extend over 10 nm. In this work we are presenting metallic nanostructures (fractal-like structure) that are put in contact with fluorophore suspension in PVA film. Since the fluorophores are uniformly distributed within the solid PVA matrix [26] it is reasonable to assume that very few fluorophores will be in direct contact with metallic nanostructure and it is safe to assume that only longer range effects will play significant role. As previously we assume that average (apparent) enhancement factor for absorption is G_A and enhancement of radiative rate is G_F . Quantum yield and fluorescence lifetime measured from uniform PVA film will be:

$$Q_Y = \frac{k_F}{k_F + k_{nr}} \quad \text{and} \quad \tau = \frac{1}{k_F + k_{nr}} \quad (1)$$

While in the presence of nanostructure will be:

$$Q_Y^m = \frac{k_F G_F}{k_F G_F + k_{nr}} \quad \text{and} \quad \tau^m = \frac{1}{k_F G_F + k_{nr}} \quad (2)$$

And observed fluorescence intensities from uniform PVA film, F and PVA film in proximity of nanostructure, F^m will be:

$$F \sim A Q_Y I_{ex} \quad \text{and} \quad F^m = A Q_Y^m G_A I_{ex} \quad (3)$$

We want to stress that this is only an average approximation of observed phenomena. When scanning a PVA film that is in the contact with metallic nanostructure we are measuring fluorescence signal (intensity) and fluorescence lifetime while excitation intensity is kept constant. The ratio of fluorescence signals and fluorescence lifetime in the presence of metal and in the metal-free place is:

$$\frac{F^m}{F} = R_F = \frac{G_F G_A (k_F + k_{nr})}{G_F k_F + k_{nr}} = \frac{Q_Y^m G_F G_A}{Q_Y} \quad (4)$$

$$\frac{\tau}{\tau^m} = R_\tau = \frac{k_F G_F + k_{nr}}{k_F + k_{nr}} \quad (5)$$

It is interesting to notice that ratio of fluorescence intensities increases as a result of both, absorption enhancement and quantum yield enhancement while ratio of fluorescence lifetime only depend on radiative rate enhancement. It is worth to consider limits for fluorescence enhancement in equation (4). If $G_F \rightarrow \infty$ quantum yield approaches 1 and fluorescence signal enhancement:

$$\frac{F^m}{F} = R_F = G_A \left(1 + \frac{k_{nr}}{k_F}\right) = G_A \left(1 + \frac{1 - Q_Y}{Q_Y}\right) \quad (6)$$

For high quantum yield molecules ($k_{nr} \ll k_F$) the enhancement is only due to the field enhancement and for lower quantum yields molecules ($k_{nr} \gg k_F$) the enhancement of quantum yield

becomes significant. Since the field enhancement (G_A) do not depend on fluorophore it is clear that to achieve highest enhancement it is beneficial to use low quantum yield fluorophores.

From equation 5 we can immediately calculate factor for quantum yield enhancement:

$$G_F = \frac{R_T + Q_Y - 1}{Q_Y} \quad (7)$$

And from equation 4 we can calculate factor for field enhancement:

$$G_A = R_F Q_Y + \frac{R_F(1-Q_Y)}{G_F} \quad (8)$$

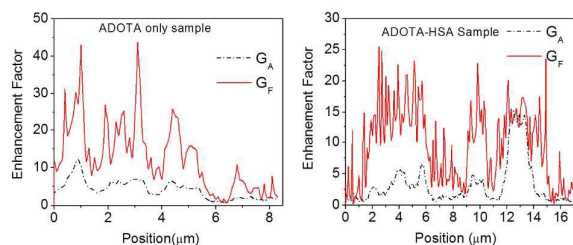


Figure 7: left panel shows the G_A and G_F values for the line drawn in figure 3B of ADOTA only sample and right panel shows the G_A and G_F values for the line drawn in figure 6B of ADOTA-HSA sample.

In our experiments, we are measuring fluorescence intensities and fluorescence lifetimes as function of the con-focal volume position scanned across the nanostructure. A low intensity regions correspond to long fluorescence lifetimes and we may safely assume these are places where we do not have enhancement (we have no nanostructure in close proximity). Using equations 6 and 7 we can recalculate to values of G_F and G_A representing average quantum yield enhancement and excitation field enhancement (Figure 7). We realize that this is a very simplified model but it clearly reflects relation between

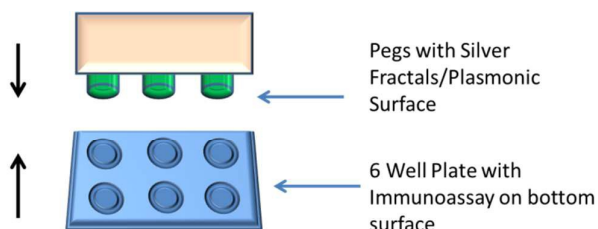


Figure 8: Proposed application of sandwich type MEF

field enhancement and quantum yield enhancement. As expected for low enhancement effect is dominated by field

enhancement and as the observed enhancement increases a contribution from quantum yield enhancement increases.

Conclusions

In conclusion, we have shown that fluorescence enhancements more than 20 times (although non-uniform) are possible using a plasmonic platform assembly where the plasmonic surface is pressed onto the fluorescent material in a sandwich fashion (Figure 8). Sørensen et al found about similar enhancement in hot spots where fractals were deposited on gold mirror and dye was deposited directly on the fractals [25]. Thus, different configuration of PP did not affect the fluorescence enhancements. This enhancement effect will depend upon the thickness of the deposited metal along with the distance of fluorophores from metallic surface and is topic of our ongoing research for this sandwich type PP. This type of PP is more convenient in terms of developing sensing/imaging applications over direct deposition of the dye onto metal surface platforms. This kind of configuration can be applied to the existing well plate or platform assays as depicted in figure 8. Fluorescence detection can be made from the bottom of the plate.

Acknowledgements

This work was supported by NIH Grants R01EB12003 and R21EB017985 (Z.G), NSF grant CBET-126408(I.G) and INFOR grant from Texas Christian University. We would like to thank Dr. Badri Maliwal for his help in HSA labelling with ADOTA and helpful comments during preparation of this manuscript and Sebastian Requena for collection of SEM images.

Notes and references

*Corresponding Author: Ignacy Gryczynski (ignacy.gryczynski@unthsc.edu), Sangram Raut (sraut@live.unthsc.edu)

- 1 Shang, L. and Dong, S., Nienhaus, G. U., Nano Today, 2011, 6, pp. 401-418.
- 2 Raut, S. and Chib, R. and Rich, R. M. and Shumilov, D. and Gryczynski, Z., Gryczynski, I., Nanoscale, 2013, 5, 3441-3446.
- 3 Raut, S. L. and Fudala, R. and Rich, R. and Kokate, R. A. and Chib, R. and Gryczynski, Z., Gryczynski, I., Nanoscale, 2014, 6, pp. 2594-2597.
- 4 Velez, O. and Tessier, P. and Lenhoff, A., Kaler, E., Nature, 1999, 401, pp. 548-548.
- 5 Demoustier-Champagne, S., Delvaux, M., Materials Science and Engineering: C, 2001, 15, pp. 269-271.
- 6 Halas, N. J. and Lal, S. and Chang, W. and Link, S., Nordlander, P., Chem. Rev., 2011, 111, pp. 3913-3961.
- 7 Xia, Y., Halas, N. J., MRS Bull., 2005, 30, pp. 338-348.
- 8 Tsuji, M. and Hashimoto, M. and Nishizawa, Y. and Kubokawa, M., Tsuji, T., Chemistry-A European Journal, 2005, 11, pp. 440-452.

- 9 Parfenov, A. and Gryczynski, I. and Malicka, J. and Geddes, C. D., Lakowicz, J. R., *The Journal of Physical Chemistry B*, 2003, 107, pp. 8829-8833.
- 10 Goldys, E. M. and Drozdowicz-Tomsia, K. and Xie, F. and Shtoyko, T. and Matveeva, E. and Gryczynski, I., *Gryczynski, Z., J. Am. Chem. Soc.*, 2007, 129, pp. 12117-12122.
- 11 Shtoyko, T. and Matveeva, E. G. and Chang, I. and Gryczynski, Z. and Goldys, E., *Gryczynski, I., Anal. Chem.*, 2008, 80, pp. 1962-1966.
- 12 Kim, W. and Safonov, V. and Shalaev, V. M., Armstrong, R., *Phys. Rev. Lett.*, 1999, 82, pp. 4811.
- 13 Podolskiy, V., Shalaev, V., *LASER PHYSICS-LAWRENCE-*, 2001, 11, pp. 26-30.
- 14 V. M. Shalaev, *Optical Properties of Nanostructured Random Media*, ed. Anonymous 2002, vol. 82,
- 15 Sørensen, T. J. and Thyrrhaug, E. and Szabelski, M. and Luchowski, R. and Gryczynski, I. and Gryczynski, Z., Laursen, B. W., *Methods and applications in fluorescence*, 2013, 1, pp. 025001.
- 16 Maliwal, B. P. and Fudala, R. and Raut, S. and Kokate, R. and Sorensen, T. J. and Laursen, B. W. and Gryczynski, Z., *Gryczynski, I., PLoS One*, 2013, 8, pp. e63043.
- 17 Gryczynski, I. and Malicka, J. and Nowaczyk, K. and Gryczynski, Z., Lakowicz, J. R., *The Journal of Physical Chemistry B*, 2004, 108, pp. 12073-12083.
- 18 Abdulhalim, I. and Karabchevsky, A. and Patzig, C. and Rauschenbach, B. and Fuhrmann, B. and Eltzov, E. and Marks, R. and Xu, J. and Zhang, F., Lakhtakia, A., *Appl. Phys. Lett.*, 2009, 94, pp. 063106.
- 19 Karabchevsky, A. and Khare, C. and Rauschenbach, B., Abdulhalim, I., *Journal of Nanophotonics*, 2012, 6, pp. 061508-1-061508-12.
- 20 Luchowski, R. and Calander, N. and Shtoyko, T. and Apicella, E. and Borejdo, J. and Gryczynski, Z., *Gryczynski, I., Journal of nanophotonics*, 2010, 4, pp. 043516-043516-17.
- 21 Matveeva, E. G. and Gryczynski, I. and Barnett, A. and Leonenko, Z. and Lakowicz, J. R., *Gryczynski, Z., Anal. Biochem.*, 2007, 363, pp. 239-245.
- 22 Barnett, A. and Matveeva, E. G. and Gryczynski, I. and Gryczynski, Z., Goldys, E. M., *Physica B: Condensed Matter*, 2007, 394, pp. 297-300.
- 23 Sokolov, K. and Chumanov, G., Cotton, T. M., *Anal. Chem.*, 1998, 70, pp. 3898-3905.
- 24 Das, P., Metiu, H., *J. Phys. Chem.*, 1985, 89, pp. 4680-4687.
- 25 Sørensen, T. J. and Laursen, B. W. and Luchowski, R. and Shtoyko, T. and Akopova, I. and Gryczynski, Z., *Gryczynski, I., Chemical physics letters*, 2009, 476, pp. 46-50.
- 26 Chib, R. and Raut, S. and Shah, S. and Grobelna, B. and Akopova, I. and Rich, R. and Sørensen, T. J. and Laursen, B. W. and Grajek, H., *Gryczynski, Z., Dyes and Pigments*, 2015, 117, pp. 16-23.
- 27 Thyrrhaug, E. and Sørensen, T. J. and Gryczynski, I. and Gryczynski, Z., Laursen, B. W., *The Journal of Physical Chemistry A*, 2013, 117, pp. 2160-2168.
- 28 Maliwal, B. P. and Fudala, R. and Raut, S. and Kokate, R. and Sorensen, T. J. and Laursen, B. W. and Gryczynski, Z., *Gryczynski, I., PLoS One*, 2013, 8, pp. e63043.
- 29 Aslan, K. and Gryczynski, I. and Malicka, J. and Matveeva, E. and Lakowicz, J. R., Geddes, C. D., *Curr. Opin. Biotechnol.*, 2005, 16, pp. 55-62.
- 30 Lakowicz, J. R., *Anal. Biochem.*, 2005, 337, pp. 171-194.
- 31 J. R. Lakowicz, *Principles of Fluorescence Spectroscopy*, ed. 2009.
- 32 Lakowicz, J. R. and Shen, Y. and D'Auria, S. and Malicka, J. and Fang, J. and Gryczynski, Z., *Gryczynski, I., Anal. Biochem.*, 2002, 301, pp. 261-277.
- 33 Malicka, J. and Gryczynski, I. and Gryczynski, Z., Lakowicz, J. R., *Anal. Biochem.*, 2003, 315, pp. 57-66.
- 34 Dragan, A. I. and Bishop, E. S. and Casas-Finet, J. R. and Strouse, R. J. and McGivney, J. and Schenerman, M. A., Geddes, C. D., *Plasmonics*, 2012, 7, pp. 739-744.
- 35 Aslan, K. and Maly, S. N., Geddes, C. D., *Chemical physics letters*, 2008, 453, pp. 222-228.
- 36 Standridge, S. D. and Schatz, G. C., Hupp, J. T., *J. Am. Chem. Soc.*, 2009, 131, pp. 8407-8409.